

Effects of zirconia precursor on gold based samples for low temperature WGS

Federica Menegazzo¹, Michela Signoretto^{1,*}, Elena Ghedini¹, Cristina Pizzolitto¹, Giuseppe Cruciani²¹ Department of Molecular Sciences and Nanosystems, Ca' Foscari University Venice and Consortium INSTM RU Venice, Via Torino 155, 30172 Venezia Mestre, Italy² Department of Physics and Earth Science, University of Ferrara, Via Saragat 1, 44122 Ferrara, Italy*corresponding author e-mail address: miky@unive.it

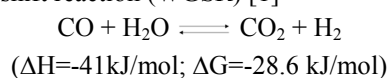
ABSTRACT

1 wt% gold-loaded zirconia and sulphated zirconia prepared from two different precursors ($ZrOCl_2 \cdot 8H_2O$ and $ZrO(NO_3)_2 \cdot 6H_2O$) were tested in the low-temperature water gas shift reaction. Samples were characterized by nitrogen adsorption analysis, sulphur content analysis, atomic absorption, X Ray-diffraction analyses (XRD) and Temperature Programmed Reductions (TPR). XRD patterns indicated a high dispersion of gold on all the samples. A strong effect of zirconia precursor on surface area, on gold dispersion and on catalytic performances has been found. Catalysts synthesized by $ZrOCl_2 \cdot 8H_2O$ precursor are more active and more stable than samples prepared by $ZrO(NO_3)_2 \cdot 6H_2O$ due to a stronger metal support interaction between gold nanoparticles and the "ex-chloride" zirconia support. Catalysts prepared on sulphated zirconia are more active and in particular more stable than catalysts supported on non-sulphated ones. On sulphated zirconia, the surface structural disorder left after sulphate removal, allows a lower mobility of gold atoms on the zirconia surface and therefore inhibits gold sintering.

Keywords: WGS; gold catalysts; zirconia; sulphated zirconia; Au/ZrO₂.

1. INTRODUCTION

The water-gas shift reaction (WGS) [1]



provides an economical route to hydrogen production and it is one of the oldest catalytic processes employed in the chemical industry. It usually proceeds in two distinct steps with two different catalysts: a high temperature process over an iron oxide promoted with chromium oxide catalyst, and a low temperature one, on a material composed of copper, zinc oxide and alumina [2]. In the last times, there has been a renewed interest in the WGS because it is one of the key steps in important applications such as pure hydrogen production for fuel-cell power systems and in the automobile exhaust processes [3]. However, in these applications they are required heterogeneous catalysts with high activity as well as good structural stability in air and in cyclic operation. These are stringent requirements not met by the commercially available low-temperature WGS catalysts [4-6].

After the pioneering work of Haruta *et al.* [7], gold nanoparticles supported on metal oxides have been shown to be very active in some important industrial reactions. As regards the WGS over supported gold catalysts, it has been the subject of numerous investigations [8-24]. It has been reported that the nature and the structure of the support strongly influence the catalytic activity and selectivity of gold-based samples. For the first time a high catalytic activity for the WGS was found using a Au/Fe₂O₃ catalyst [8], then Au/TiO₂ [25], Au/ZnO [26], Au/CeO₂ [27,28], Au/ThO₂ [29] catalysts have also been investigated. It has been found that mesoporous zirconia with high surface area and uniform pore size distribution, is a very efficient support of gold-based catalyst for the WGS reaction [30]. Zirconia is of particular

interest since by the addition of different dopants it is possible to control different properties such as for example surface area, porosity, redox properties, surface acidity and/or basicity. In particular sulphated zirconia [31] has been the subject of many investigations due to its characteristics: it causes not only modifications of the acid properties, but affects also surface features since sulphates retard crystallization, stabilize the tetragonal phase, improve surface area and pore size. Firstly, it has been published a patent [32] related to highly dispersed gold on sulphated zirconia under water gas-shift conditions, claiming high activity and stability of the novel catalyst. We have previously tested gold over zirconia and sulphated zirconia catalysts in the low temperature water-gas shift reaction [33-36]. Activity data have shown that highly dispersed gold on zirconia catalysts are much more active than the gold on titania Reference catalyst, where nanoparticles are present. Moreover, gold catalysts over sulphated zirconia showed higher activities than samples on plain zirconia, due to the promotion of zirconia to a higher specific surface area that leads to a better dispersion of gold nanoparticles on the surface. In fact, a very good relationship between catalytic activity and chemisorption data has been highlighted.

In the present work we have investigated low-temperature WGS reactions on gold-loaded zirconia and sulphated zirconia prepared from two different precursors ($ZrOCl_2 \cdot 8H_2O$ and $ZrO(NO_3)_2 \cdot 6H_2O$). The aim was to improve the knowledge of these catalytic systems for the low temperature water gas-shift reaction. In fact, the effect of different zirconia precursor could influence morphological and structural properties of the final material, leading to different catalytic performances as for activity, selectivity and stability.

2. EXPERIMENTAL SECTION

2.1. Catalyst preparation. Zirconia supports were prepared from two different precursors ($ZrOCl_2 \cdot 8H_2O$ (Fluka) and

$ZrO(NO_3)_2 \cdot 6H_2O$ (Fluka)), that were used as received for sample synthesis.

A first support ($Zr(OH)_4$ 1) was prepared by precipitation from $ZrOCl_2$ at constant pH (pH=8.6), aged under reflux conditions for 20 hours [37,38], washed free from chloride ($AgNO_3$ test) and dried at 383 K overnight. The other one ($Zr(OH)_4$ 2) was prepared by precipitation from $ZrO(NO_3)_2 \cdot 6H_2O$ at constant pH (pH=8.6) and aging at ambient temperature for 90 minutes [32]. After filtration and washing, it was dried at 383 K overnight. Part of the two supports was sulphated with $(NH_4)_2SO_4$ (Merck) by incipient wetness impregnation (2.5 wt% SO_4^{2-}/ZrO_2). Then not sulphated (Z1 and Z2) and sulphated (SZ1 and SZ2) supports were heated up to 923 K slowly over 7 hours in flowing air (50 mL/min STP) and kept at this temperature for 6 hours, followed by slow cooling to ambient temperature [32]. Gold was deposited on the calcined supports by deposition precipitation at pH=8.6 with Na_2CO_3 (1M) (Riedel-de Haen) and $HAuCl_4$ aqueous solutions to give a nominal 0.8 % wt Au loaded catalyst. After filtration, samples were finally dried at 310 K for 15 hour.

2.2. Methods. Surface area and pore size distributions were obtained from N_2 adsorption/desorption isotherm at 77 K (using a Micromeritics ASAP 2000 Analyser). Calcined samples (400 mg) were pre-treated at 573 K for 2 hours under vacuum, while noncalcined samples (300 mg) were pre-treated at 373 K for 2 hours under vacuum. Surface area was calculated from the N_2 adsorption isotherm by the BET equation, and pore size distribution was determined by the BJH method also applied on the adsorption branch [39]. Total pore volume was taken at $p/p_0 = 0.99$.

The amount of sulphate was determined by ion chromatography (IEC) after dissolution of the materials [40]. All concentrations were calculated as the average of two independent sample analyses, and each analysis included two chromatographic determinations.

3. RESULTS SECTION

3.1. N_2 physisorption analyses. N_2 physisorption data are reported in Table 1, while the corresponding isotherms are shown in Figure 1. In particular, N_2 physisorption isotherms of zirconium hydroxides (section a), calcined materials (section b) and sulphated calcined zirconia (section c) are shown in Figure 1. All samples show type IV isotherms with hysteresis loop typical of mesoporous materials. Not calcined, not doped zirconia precursor prepared with $ZrOCl_2 \cdot 8H_2O$ is mesoporous (BJH mean pore size 4.8 nm) but shows a high fraction of microporosity and a very high BET surface area ($370 \text{ m}^2 \text{ g}^{-1}$). The N_2 physisorption isotherm of hydroxide prepared with $ZrO(NO_3)_2 \cdot 6H_2O$ (Figure 1, section a) presents a different form with respect the isotherm previously discussed: the hysteresis loop typical of mesoporous materials starts at a value of $p/p_0 = 0.4$ and it is flattened. As reported in Table1, the N_2 total adsorbed volume, BET surface area and the mean pore diameter are lower than the value reported for the hydroxide prepared with $ZrOCl_2 \cdot 8H_2O$.

The fragile amorphous structure of $Zr(OH)_4$ 1 almost collapsed after calcination to produce in the case of non doped zirconia (Z1) a mesoporous material with low surface area ($\cong 50 \text{ m}^2 \text{ g}^{-1}$) and mean pore size around 23 nm.

Actual metal loading was determined by atomic absorption spectroscopy after microwave disgregation of the samples (50 mg).

Temperature programmed reductions (TPR) were carried out in a home-made equipment: samples (100 mg) were heated at 10 K/min from 300 K to 1300 K in a 5% H_2/Ar reducing mixture (40 mL min^{-1} STP).

X-ray powder diffraction (XRD) patterns were measured by a Bruker D8 Advance diffractometer equipped with a Si(Li) solid state detector (SOL-X) and a sealed tube providing Cu $K\alpha$ radiation. Measuring conditions were 40 kV x 40 mA. Apertures of divergence, receiving and detector slits were 1° , 1° , and 0.3° respectively. Data scans were performed in the 2θ ranges $15-55^\circ$ and $35-40^\circ$ with 0.02° step size and counting times of 3 s step^{-1} and 10 s step^{-1} , respectively.

2.3. Catalytic activity measurement. WGSR was performed in a fixed-bed flow reactor at atmospheric pressure and in the temperature range from 523 to 423 K. The following conditions were applied: 9400 h^{-1} of space velocity, 0.5 cm^3 of catalyst bed volume (35-50 mesh) diluted to 1.5 cm^3 with silica (35-50 mesh), the feed mixture contained 1.9 vol.% CO , 39.7 vol.% H_2 , 9.5 vol.% CO_2 , 11.4 vol.% N_2 , 37.5 vol.% H_2O . The catalysts were previously subjected to a slow thermal activation (50 K h^{-1}) in nitrogen up to 523 K and kept at this temperature for 17 hours (N_2 flow = 50 mL min^{-1}). After 21 hours of WGSR, samples were reactivated in hydrogen (H_2 flow = 50 mL min^{-1}) up to 493 K and tested in the WGSR for other 21 hours. The progress of the reaction was followed by gas-chromatographic analyses of the converted mixture at the reactor outlet.

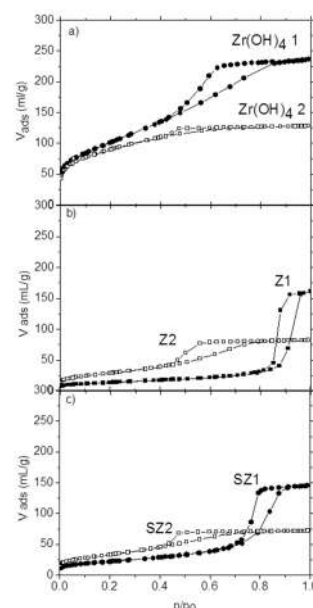


Figure 1: N_2 physisorption isotherms of hydroxides (section a), zirconia (section b) and sulphated zirconia (section c) prepared with $ZrOCl_2 \cdot 8H_2O$ (full markers) and with $ZrO(NO_3)_2 \cdot 6H_2O$ (empty markers).

On the contrary, sulphates doping yielded material (SZ1) retains a higher surface area ($\cong 80 \text{ m}^2 \text{ g}^{-1}$) and presents a structure with mean pore size around 11 nm. Also for the supports prepared with $\text{ZrO}(\text{NO}_3)_2 \cdot 6\text{H}_2\text{O}$, sulphates doped material (SZ2) retains a higher surface area ($\cong 121 \text{ m}^2 \text{ g}^{-1}$) than the non-doped calcined zirconia (Z2) ($\cong 105 \text{ m}^2 \text{ g}^{-1}$).

Therefore, in agreement with literature data, the presence of sulphates leads to an increase in surface area for both the zirconia precursors. In fact it is well known that the presence of sulphates ions on the support is crucial during the calcination step, as sulphate are able to stabilize the metastable tetragonal zirconia phase which has a higher surface area than the monoclinic phase [41,42].

On the contrary, a negative effect of chlorine during calcination is evident: a higher sintering of the material occurs for zirconia synthesized by $\text{ZrOCl}_2 \cdot 8\text{H}_2\text{O}$. This is in agreement with previous findings [43] about the BET area of pure zirconia samples, which depends on the precursor used for the preparation, and where the largest surface area is obtained with the zirconyl nitrate precursor.

Table 1. Surface features of supports.

sample	Zirconia precursor	SSA m^2/g	pore volume cm^3/g	pore diameter nm	wt%
Zr(OH) ₄ 1	ZrOCl ₂ ·8H ₂ O	370	0.37	4.8	//
Z1	ZrOCl ₂ ·8H ₂ O	50	0.25	22.8	//
SZ1	ZrOCl ₂ ·8H ₂ O	81	0.23	10.7	2.1
Zr(OH) ₄ 2	ZrO(NO ₃) ₂ ·6H ₂ O	321	0.20	3.7	//
Z2	ZrO(NO ₃) ₂ ·6H ₂ O	105	0.13	5.0	//
SZ2	ZrO(NO ₃) ₂ ·6H ₂ O	121	0.11	4.1	2.1

Surface area and porosity are very similar for the supports and the corresponding catalysts, proving that they are not modified by the technique of deposition precipitation that we have used to introduce gold on the support.

In Table 1 sulphates loading on supports after calcination are also reported. Both Zr(OH)₄ 1 and Zr(OH)₄ 2 samples were impregnated in amounts necessary to yield a 2.5 wt% anion loading and the effective amount of sulphates in both the final calcined supports (SZ1 and SZ2) is about 2.1 wt%. On the contrary, the corresponding final catalysts (AuSZ1 and AuSZ2) do not contain sulphates anymore [33]. In fact, the methodology of gold deposition precipitation on the support has been carried out at a basic pH, and the detachment of sulphate groups has occurred. In fact, we had previously demonstrated the complete dissolution of sulphates from a zirconia matrix under basic solution [40].

3.2. Temperature Programmed Reductions (TPR). Figure 2 shows the TPR analyses for zirconia samples prepared with $\text{ZrOCl}_2 \cdot 8\text{H}_2\text{O}$ (a) and with $\text{ZrO}(\text{NO}_3)_2 \cdot 6\text{H}_2\text{O}$ (b). TPR profiles of Z1 and Z2 supports don't show any peaks. On the contrary, TPR profiles of Z1S and Z2S materials present at about 920 K a peak. The latter, as shown in the mass signal, is due to sulphate reduction mainly to SO_2 ($m/e=48$; $m/e=64$) and in part to H_2S ($m/e=34$) [38]. This peak disappears in the analyses of gold containing samples, indicating that final catalysts do not contain sulphates. In fact, as already discussed, deposition precipitation of the metal at a basic pH allows sulphates disappearance. It is interesting to note that there aren't peaks related to gold reduction for any catalyst, meaning that in these samples the metal is completely reducible already at room temperature. In fact mass

spectroscopy shows that the two small peaks located at about 450 K and 820 K are due to $m/e=44$ and $m/e=28$, and not to hydrogen consumption, and they are probably due to residual carbonate after gold introduction.

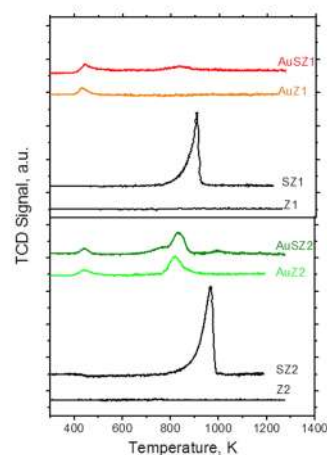


Figure 2. TPR profiles of calcined supports and catalysts.

3.3. XRD. X-ray diffraction patterns for the four calcined supports are reported in Figure 3 (section a). It is possible to see that different preparation methods result in completely different samples. The “ex-chloride” zirconia samples are crystalline predominantly in the monoclinic phase, while in the “ex-nitrate” zirconia catalysts the majority of the material is in the tetragonal structure. This is in agreement with the previously discussed BET area, since the monoclinic phase has lower surface area than the tetragonal phase.

The crystalline structure of the gold-based catalysts is the same of the corresponding support (Figure 3, section b). Besides for these samples it is interesting to note the absence of any peaks related to Au, strongly suggesting a high dispersion of gold on both zirconia supports, either sulphated or not.

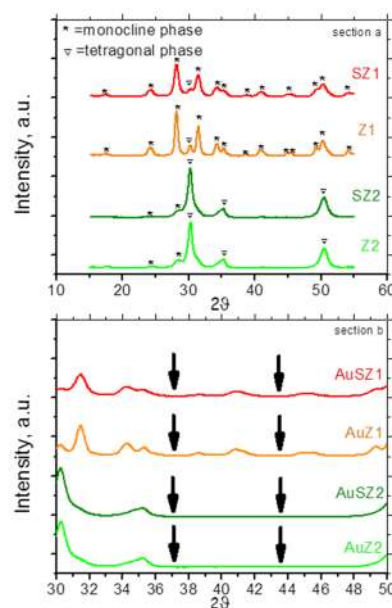


Figure 3. XRD patterns of calcined supports (section a) and catalysts (section b).

3.5. Kinetic data. Table 2 reports the WGS reaction conversion results at 523 K. Both zirconia supports, either sulphated or not, exhibited no activity under the experimental conditions and after different activations, indicating that gold is the real active phase of the process. First of all it is interesting to note that both the “ex-

chloride” catalysts present higher activity than the corresponding “ex-nitrate” catalysts. This can be reasonably ascribed to a stronger metal support interaction between gold nanoparticles and the “ex-chloride” zirconia support. In addition, it has been found that samples prepared on sulphated zirconia are more active than catalysts supported on non-sulphated ones. We have already shown [35,36] even if sulphates are not present in the final catalyst, they act in the synthesis step and their addition to zirconia leads to higher gold dispersion. This is due to the positive role of SO_4^- groups that address the deposition of Au in the form of highly dispersed clusters in close contact with the support. In fact, we have previously demonstrated that the $\text{Au}(\text{OH})_3$ species react with the OH groups of the zirconia surface. In the sulphated samples, the reacting OH sites are mainly produced by the removal of the sulphate groups, i.e. while the pH is raising. These “nascent” OH may react with the gold complexes in solution, forming quite isolated gold grafted species at the surface of sulphated support and, after calcination, very small Au_2O_3 clusters. Therefore, the higher conversion of samples prepared on sulphated zirconia is reasonably due to higher dispersion of these samples.

Table 2: Metal content by A.A., apparent activation energies and conversions data at 523 K.

Sample	Au wt%	E_a , Kcal/mol	Conversion at 523 K, %
AuZ1	0.77	6.5	80.1
AuSZ1	0.79	9.7	82.2
AuZ2	0.71	6.1	70.5
AuSZ2	0.77	7.1	74.7

In Table 2 the apparent activation energies (E_a) for all the samples are also reported. They have been calculated from the Arrhenius-type plot for rate constant k of the reaction, determined by assuming a first order reaction with respect to CO [33]. This is represented also in Figure 4. As it can be seen, the value of E_a for all the gold on zirconia samples are in the range 9.7 - 6.1 Kcal mol^{-1} . Such values are similar to that determined for Au/ZrO_2 [33] and Au/CeO_2 catalysts [4]. Besides in this work we have investigated the stability of the gold-based catalysts. Results are

4. CONCLUSIONS

A strong effect of zirconia precursor on surface area, on gold dispersion and on catalytic performances has been found. Catalysts synthesized by $\text{ZrOCl}_2 \cdot 8\text{H}_2\text{O}$ precursor are more active and more stable than samples prepared by $\text{ZrO}(\text{NO}_3)_2 \cdot 6\text{H}_2\text{O}$ due to the stronger metal support interactions between gold nanoparticles and the “ex-chloride” zirconia support. Catalysts prepared on

5. REFERENCES

- [1] Reddy G. K., Smirniotis P. G., in “Water-gas shift reaction - Research Developments and Applications”, Elsevier, Chapter 3 Low-temperature WGS reaction, 47-100, **2015**.
- [2] Li Y., Fu Q., Flytzani-Stephanopoulos M., Low-temperature water-gas shift reaction over Cu- and Ni-loaded cerium oxide catalysts, *Applied Catalysis B Environmental*, 27, 179, **2000**.
- [3] Andreeva D., Low temperature water gas shift over gold catalysts, *Gold Bulletin*, 35, 82, **2002**.
- [4] Fu Q., Saltsburg H., Flytzani-Stephanopoulos M., Active Nonmetallic Au and Pt Species on Ceria-Based Water-Gas Shift Catalysts, *Science*, 301, 935, **2003**.
- [5] Kaftan A., Kusche M., Laurin M., Wasserscheid P., Libuda J., KOH-promoted $\text{Pt}/\text{Al}_2\text{O}_3$ catalysts for water gas shift and methanol steam

shown in Figure 5. Both catalysts supported on zirconia prepared with $\text{ZrOCl}_2 \cdot 8\text{H}_2\text{O}$ are more stable than samples obtained by $\text{ZrO}(\text{NO}_3)_2 \cdot 6\text{H}_2\text{O}$. Again, this can be due to a stronger metal support interaction between gold nanoparticles and the “ex-chloride” zirconia support.

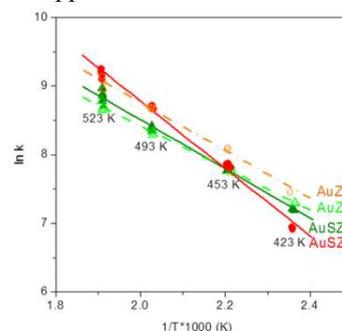


Figure 4: Comparison of catalytic activity on fresh samples. (○) AuZ1; (●) AuSZ1; (△) AuZ2; (▲) AuSZ2.

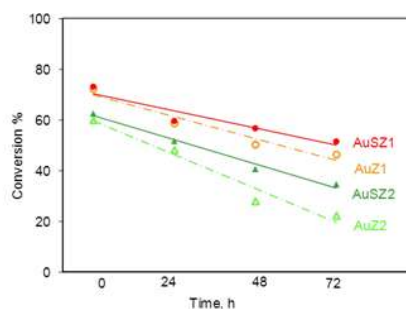


Figure 5: Comparison of stability on various samples: (○) AuZ1; (●) AuSZ1; (△) AuZ2; (▲) AuSZ2. (Conversions are calculated at 493 K).

Under LT-WGSR conditions, moreover, both samples prepared on sulphated zirconia are more stable than the corresponding catalysts over non-sulphated support (Figure 6). In particular, the AuSZ1 sample lost a 17 % less than the corresponding AuZ1 catalyst, while the AuSZ2 sample lost a 29 % less than the AuZ2 catalyst. This is possibly a consequence of the lower surface mobility of gold on more disordered surfaces. On sulphated zirconia, the surface structural disorder left after sulphate removal, allows a lower mobility of gold atoms on the zirconia surface and therefore inhibits gold sintering [26].

sulphated zirconia are more active and in particular more stable than catalysts supported on non-sulphated ones. On sulphated zirconia, the surface structural disorder left after sulphate removal, allows a lower mobility of gold atoms on the zirconia surface and therefore inhibits gold sintering.

reforming: An operando DRIFTS-MS study, *Applied Catalysis B: Environmental*, 201, 169-181, **2017**.

[6] Miao D., Cavusoglu G., Lichtenberg H., Yu J., Xu H., Grunwaldt J., Goldbach A., Water-gas shift reaction over platinum/strontium apatite catalysts, *Applied Catalysis B: Environmental*, 202, 587-596, **2017**.

[7] Haruta M., Kobayashi T., Sano H., Yamada N., Novel gold catalysts for the oxidation of carbon monoxide at a temperature far below 0 °C, *Chemistry Letters*, 405, **1987**.

[8] Andreeva D., Idakiev V., Tabakova T., Andreev A., Low-Temperature Water-Gas Shift Reaction over $\text{Au}/\alpha\text{-Fe}_2\text{O}_3$, *Journal of Catalysis*, 158, 354-355, **1996**.

[9] Santos J.L., Reina T.R., Ivanova S., Centeno M.A., Odriozola J.A., Gold promoted $\text{Cu}/\text{ZnO}/\text{Al}_2\text{O}_3$ catalysts prepared from hydrotalcite

precursors: Advanced materials for the WGS reaction, *Applied Catalysis B Environmental*, 201, 310-317, **2017**.

[10] Gamboa-Rosales N.K., Ayastuy J.L., Gutiérrez-Ortiz M.A., Effect of Au in Au–Co₃O₄/CeO₂ catalyst during oxygen-enhanced water gas shift, *International Journal of Hydrogen Energy*, doi.org/10.1016/j.ijhydene.2016.05.237, **2016** (in press).

[11] Nguyen-Phan T., Baber A. E., Rodriguez J.A., Senanayake S. D., Au and Pt nanoparticle supported catalysts tailored for H₂ production: From models to powder catalysts, *Applied Catalysis A General*, 518, 18-47, **2016**.

[12] Hakeem A. A., Zhao Z., Kapteijn F., Makkee M., Revisiting the synthesis of Au/TiO₂ P25 catalyst and application in the low temperature water–gas shift under realistic conditions, *Catalysis Today*, 244, 19-28, **2015**.

[13] Hakeem A. A., Rajendran J., Kapteijn F., Makkee M., Promotion or additive activity? The role of gold on zirconia supported iron oxide in high temperature water-gas shift, *Journal of Molecular Catalysis A: Chemical*, 420, 115-123, **2016**.

[14] Grinter D.C., Park J.B., Agnoli S., Evans J., Hrbek J., Stacchiola D.J., Senanayake S.D., Rodriguez J.A., Water–gas shift reaction over gold nanoparticles dispersed on nanostructured CeO_x–TiO₂(110) surfaces: Effects of high ceria coverage, *Surface Science*, 650, 34-39, **2016**.

[15] González-Castaño M., Reina T. R., Ivanova S., Martínez Tejada L.M., Centeno M.A., Odriozola J.A., O₂-assisted Water Gas Shift reaction over structured Au and Pt catalysts, *Applied Catalysis B Environmental*, 185, 337-343, **2016**.

[16] Özyöntüm G. N., Yildirim R., Water gas shift activity of Au–Re catalyst over microstructured cordierite monolith wash-coated by ceria, *International Journal of Hydrogen Energy*, 41, 12, 5513-5521, **2016**.

[17] Vindigni F., Manzoli M., Tabakova T., Idakiev V., Boccuzzi F., Chiorino A., Gold catalysts for low temperature water-gas shift reaction: Effect of ZrO₂ addition to CeO₂ support, *Applied Catalysis B Environmental*, 125, 507-515, **2013**.

[18] Tabakova T., Boccuzzi F., Manzoli M., Sobczak J.W., Idakiev V., Andreeva D., Effect of synthesis procedure on the low-temperature WGS activity of Au/ceria catalysts, *Applied Catalysis B Environmental*, 49, 73-81, **2004**.

[19] Fu Q., Deng W., Saltsburg H., Flytzani-Stephanopoulos M., Activity and stability of low-content gold–cerium oxide catalysts for the water–gas shift reaction, *Applied Catalysis B Environmental*, 56, 57-68, **2005**.

[20] Ilieva L., Tabakova T., Pantaleo G., Ivanov I., Zanella R., Paneva D., Velinov N., Sobczak J.W., Lisowski W., Avdeev G., Venezia A.M., Nano-gold catalysts on Fe-modified ceria for pure hydrogen production via WGS and PROX: Effect of preparation method and Fe-doping on the structural and catalytic properties, *Applied Catalysis A General*, 467, 76-90, **2013**.

[21] Tabakova T., Ilieva L., Ivanov I., Zanella R., Sobczak J.W., Lisowski W., Kaszkur Z., Andreeva D., Influence of the preparation method and dopants nature on the WGS activity of gold catalysts supported on doped by transition metals ceria, *Applied Catalysis B Environmental*, 136-137, 70-80, **2013**.

[22] Zhang Y., Zhan Y., Chen C., Cao Y., Lin X., Zheng Q., Highly efficient Au/ZrO₂ catalysts for low-temperature water–gas shift reaction: Effect of pre-calcination temperature of ZrO₂, *International Journal of Hydrogen Energy*, 37, 17, 12292-12300, **2012**.

[23] Andreeva D., Ivanov I., Ilieva L., Abrashev M.V., Gold catalysts supported on ceria and ceria–alumina for water-gas shift reaction, *Applied Catalysis A General*, 302, 127-132, **2006**.

[24] Jacobs G., Ricote S., Patterson P. M., Graham U. M., Dozier A., Khalid S., Rhodus E., Davis B. H., Low temperature water-gas shift: Examining the efficiency of Au as a promoter for ceria-based catalysts prepared by CVD of a Au precursor, *Applied Catalysis A General*, 292, 229-243, **2005**.

[25] Sakurai H., Ueda A., Kobayashi T., Haruta M., Low-temperature water–gas shift reaction over gold deposited on TiO₂, *Chemical Communications*, 271-272, **1997**.

[26] Tabakova T., Idakiev V., Andreeva D., Mitov I., Influence of the microscopic properties of the support on the catalytic activity of Au/ZnO, Au/ZrO₂, Au/Fe₂O₃, Au/Fe₂O₃–ZnO, Au/Fe₂O₃–ZrO₂ catalysts for the WGS reaction, *Applied Catalysis A General*, 202, 91-97, **2000**.

[27] Andreeva D., Idakiev V., Tabakova T., Ilieva L., Falaras P., Bourlinos A., Travlos A., Low-temperature water-gas shift reaction over Au/CeO₂ catalysts, *Catalysis Today*, 72, 51-57, **2002**.

[28] Fu Q., Weber A., Flytzani-Stephanopoulos M., *Catalysis Letters*, 77, 87, **2001**.

[29] Tabakova T., Idakiev V., Tenchev K., Boccuzzi F., Manzoli M., Chiorino A., *Applied Catalysis B Environmental*, 63, 94, **2006**.

[30] Idakiev V., Tabakova T., Naydenov A., Yuan Z.-Y., Su B.-L., *Applied Catalysis B Environmental*, 63, 178, **2006**.

[31] Moseley F., Dyer P.N., US 4, 336, 240, **1982**.

[32] Kuperman A., Moir M., WO 2005 005032, **2005**.

[33] Menegazzo F., Pinna F., Signoretto M., Trevisan V., Boccuzzi F., Chiorino A., Manzoli M., Highly dispersed gold on zirconia: characterization and activity in LT-WGS tests, *ChemSusChem*, 1, 320-326, **2008**.

[34] Zane F., Trevisan V., Pinna F., Signoretto M., Menegazzo F., Investigation on gold dispersion of Au/ZrO₂ catalysts and activity in the low-temperature WGS reaction, *Applied Catalysis B Environmental*, 89, 303-308, **2009**.

[35] Manzoli M., Boccuzzi F., Trevisan V., Menegazzo F., Signoretto M., Pinna F., Au/ZrO₂ catalysts for LT-WGS: active role of sulfates during gold deposition, *Applied Catalysis B Environmental*, 96, 28-33, **2010**.

[36] Signoretto M., Menegazzo F., Trevisan V., Pinna F., Manzoli M., Boccuzzi F., Investigation on the Stability of Supported Gold Nanoparticles *Catalysts*, 3, 656-670, **2013**.

[37] Melada S., Signoretto M., Somma F., Pinna F., Cerrato G., Meligrana G., Morterra C., *Catalysis Letters*, 94, 193, **2004**.

[38] Signoretto M., Melada S., Pinna F., Polizzi S., Cerrato G., Morterra C., *Microporous Mesoporous Materials*, 81, 19, **2005**.

[39] Gregg S.J., Sing K.S.W., Adsorption, Surface Area and Porosity – 2nd ed., Academic Press, p. 111, **1982**.

[40] Sarzanini C., Sacchero G., Pinna F., Signoretto M., Cerrato G., Morterra C., Amount and nature of sulfates at the surface of sulfate-doped zirconia catalysts, *Journal of Material Chemistry*, 5, 353, **1995**.

[41] Morterra C., Cerrato G., Pinna F., Signoretto M., *Journal of Catalysis*, 157, 109, **1995**.

[42] Ward D.A., Ko E.I., *Journal of Catalysis*, 150, 18, **1994**.

[43] Rossignol S., Madier Y., Duprez D., Preparation of zirconia–ceria materials by soft chemistry, *Catalysis Today*, 50, 261-270, **1999**.

6. ACKNOWLEDGEMENTS

We thank Mrs. Tania Fantinel for technical assistance.

© 2016 by the authors. This article is an open access article distributed under the terms and conditions of the Creative Commons Attribution license (<http://creativecommons.org/licenses/by/4.0/>).